

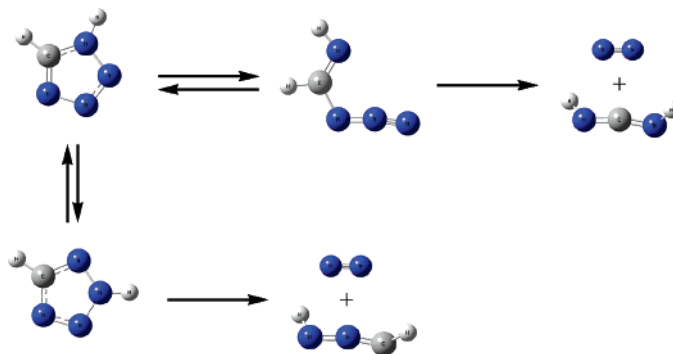
Retro-[3 + 2]-Cycloaddition Reactions in the Decomposition of Five-Membered Nitrogen-Containing Heterocycles

Gabriel da Silva^{†,‡} and Joseph W. Bozzelli^{*,†}

Department of Chemistry and Environmental Science, New Jersey Institute of Technology, Newark, New Jersey 07102, and Department of Chemical and Biomolecular Engineering, University of Melbourne, Victoria 3010, Australia

bozzelli@njit.edu

Received September 10, 2007



Nitrogen-containing heterocycles form the basis for a new generation of high-energy density materials, and they serve as model compounds for nitrogen-containing fuels, such as coal and biomass, and they form the backbone of ionic liquids. A novel retro-[3 + 2]-cycloaddition to a three-membered diene and a two-membered dienophile, analogous to a retro-Diels–Alder reaction, may constitute an important initial reaction step in the thermal decomposition of these heterocyclic compounds. We investigate the kinetics and thermodynamics of these reactions for the heterocycles pyrrole, pyrazole, imidazole, 1,2,3-triazole, 1,2,4-triazole, 1,2,5-triazole, 1,3,4-triazole, 1*H*-tetrazole, and 2*H*-tetrazole, using theoretical computational chemistry. The retro-cycloadditions are shown to form one of the three-membered products: hydrazoic acid (NH=N=N), nitrilimine (NH=N=CH), carbodiimide (NH=C=NH), or ketenimine (NH=C=CH₂) plus one of the two-membered products acetylene, hydrogen cyanide, or N₂. Accurate enthalpies of formation are calculated for the reaction products using the high-level W1 computational protocol, providing the previously undetermined enthalpy values of 70.09, 88.75, 35.03, and 44.28 kcal mol⁻¹ for hydrazoic acid, nitrilimine, carbodiimide, and ketenimine, respectively. We apply a variable-order form of the Marcus equation to the dissociation reactions in correlating the enthalpy of reaction with the activation enthalpy. Typical molecular elimination reactions from the heterocycles proceed with an intrinsic activation enthalpy of 36.8 kcal mol⁻¹ and intrinsic activation free energy of 42.1 kcal mol⁻¹. However, dissociation reactions resulting in the formation of either NH=C=NH or NH=C=CH₂ demonstrate intrinsic barriers ca. 30 kcal mol⁻¹ higher, as a result of a concerted intramolecular hydrogen shift. Rate constants calculated between 300 and 3000 K indicate that the proposed dissociation reactions should be important in the decomposition of tetrazole and 1,2,3-triazole. This is confirmed by comparison with available experimental data. Decomposition of 1,2,4-triazole to HCN + nitrilimine may also be important at high temperatures. From extrapolation of our Marcus equation relationship, we predict pentazole to decompose to N₂ + NHNN with an activation enthalpy of 19.5 kcal mol⁻¹ and a half-life of only 14 s at 298 K.

Introduction

There has been much interest of late in high nitrogen content heterocycles, due to the possible applications of these com-

pounds as the next generation of high-energy density materials. These materials possess relatively large enthalpies of formation and react to form benign N₂, among other products. The five-membered nitrogen-containing heterocycles and their various substituted derivatives are one such group of compounds. Of particular interest are imidazole salts and the triazoles and tetrazoles. There have been attempts to isolate pentazole (*cyclo-*

* To whom correspondence should be addressed. Phone: + 973-596-3459. Fax: + 973-596-3586. E-mail: bozzelli@njit.edu.

[†] New Jersey Institute of Technology.

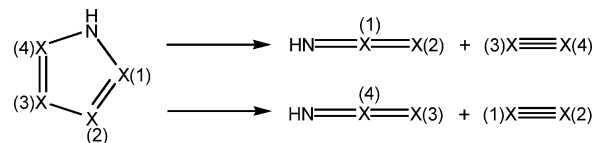
[‡] University of Melbourne.

(N₅H), and successful synthesis of the pentazolide ion has been reported.¹ Imidazole (*cyclo*-N₂C₃H₄) plays an important role as the backbone for ionic liquids, which also have possible applications as high-energy density materials.² Understanding the conditions under which traditional imidazole-based ionic liquids thermally degrade is also of importance.³

In addition to their use as energetic materials, nitrogen-containing heterocycles have been proposed as model compounds for solid fuels such as biomass and coal.^{4,5} Understanding the combustion kinetics of these compounds helps us model the evolution of unwanted NO_x from nitrogen-containing solid fuels. The reaction kinetics of pyrrole and pyrazole (which are the dominant nitrogen-containing functional groups in coals) are relatively well-studied, both experimentally^{5,6} and theoretically.⁷ The higher nitrogen content heterocycles and their derivatives may find use as biomass model compounds, as biomass will typically contain a more diverse array of organic functional groups than coal. While there has been some experimental work on the thermal decomposition of the higher nitrogen content heterocycles, their thermochemistry and decomposition mechanisms are relatively poorly known, with little theoretical support for empirical or semiempirical reaction pathways. The thermal decomposition of tetrazole has been shown to predominantly yield HCN plus NHNN, with other products including NH₃, CH₄, and C₂H₂ also produced at higher temperatures.⁸ 1,2,3-Triazole decomposes to CH₃CN, with HCN and NH₃;^{10,11} MNDO calculations support formation of a cyclic intermediate in the initial stages of this process.¹¹

High nitrogen content heterocycles can be difficult to study experimentally, due to their relative instability. As such, computational methods have been widely employed to calculate

SCHEME 1. Retro-[3 + 2]-Cycloaddition Reactions of the Five-Membered Nitrogen-Containing Heterocycles, Where X = CH or N



thermochemical properties for the nitrogen-containing heterocycles and for their reaction products.¹⁰ In contrast, relatively little attention has been paid to the reaction kinetics of these high nitrogen content materials. da Silva et al.⁴ calculated bond dissociation energies for each of the N–H and C–H bonds in the five-membered nitrogen-containing heterocycles, and in all cases, they identified the N–H bonds to be the weakest, with BDEs of between 96 and 116 kcal mol⁻¹. In general, the N–H BDEs were found to increase with increasing nitrogen content of the heterocycle. All C–H BDEs in the heterocycles were found to be high, between 117 and 124 kcal mol⁻¹, and varied relatively little between molecules. It was proposed by da Silva et al.⁴ that abstraction of the N–H hydrogen atom would be an important initial step in the combustion of the five-membered nitrogen-containing heterocycles.

We now hypothesize that an important first step in the decomposition of the five-membered nitrogen-containing heterocycles might be a retro-[3 + 2]-cycloaddition (RCA), in addition to the currently considered reactions, such as N–H and C–H hydrogen abstractions and ring opening with subsequent bond dissociation reactions. The RCA reactions of the five-membered nitrogen-containing heterocycles are depicted in Scheme 1. Here, the two-membered product is found to be one of acetylene, hydrogen cyanide, or N₂, and the possible three-membered products are N•H–CH=C•H, N•H–CH=N•, NH=N⁺=CH⁻, and NH=N⁺=N⁻. In our work, we find that the N•H–CH=C•H and N•H–CH=N• diradicals are unstable, and molecular elimination incorporates a concerted intramolecular hydrogen shift resulting in formation of the closed-shell species NH=C=CH₂ and NH=C=NH. Similar dissociation reactions with concerted hydrogen shifts have been proposed in the decomposition of a series of azido compounds, including azidoacetate and azidoacetamide.^{12,13} It can be seen that each of the stable three-membered dissociation products possesses a diene structure, or contributing diene resonance structure. Our retro-[3 + 2]-cycloadditions are therefore analogous to retro-

(1) (a) Butler, R. N.; Stephens, J. C.; Burke, L. A. *Chem. Commun.* **2003**, 1016. (b) Hammerl, A.; Klapötke, T. M. *Inorg. Chem.* **2002**, *41*, 906. (c) Östmark, H.; Wallin, S.; Brinck, T.; Carlqvist, P.; Claridge, R.; Hedlund, E.; Yudina, L. *Chem. Phys. Lett.* **2003**, *379*, 539. (d) Vij, A.; Pavlovich, J. G.; Wilson, W. W.; Vij, V.; Christie, K. O. *Angew. Chem., Int. Ed.* **2002**, *41*, 3051.

(2) For example, see: Zorn, D. D.; Boatz, J. A.; Gordon, M. S. *J. Phys. Chem. B* **2006**, *110*, 11110.

(3) Baranyai, K. J.; Deacon, G. B.; MacFarlane, D. R.; Pringle, J. M.; Scott, J. L. *Aust. J. Chem.* **2004**, *57*, 145.

(4) da Silva, G.; Moore, E. E.; Bozzelli, J. W. *J. Phys. Chem. A* **2006**, *110*, 13979.

(5) (a) Ikeda, E.; Mackie, J. C. *J. Anal. Appl. Pyrolysis* **1995**, *34*, 47. (b) Wójtowicz, M. A.; Pels, J. R.; Mouljin, J. A. *Fuel* **1995**, *74*, 507. (c) Babich, I. V.; Seshan, K.; Lefferts, L. *Appl. Catal. B* **2005**, *59*, 205. (d) Thomas, K. M. *Fuel* **1997**, *76*, 457.

(6) (a) Mackie, J. C.; Colket, M. B., III; Nelson, P. F.; Esler, M. *Int. J. Chem. Kinet.* **1991**, *23*, 733. (b) Bruinsma, O. S. L.; Tromp, P. J. J.; de Sauvage Nolting, H. J. J.; Mouljin, J. A. *Fuel* **1988**, *67*, 334. (c) Alzueta, M. U.; Tena, A.; Bilbao, R. *Combust. Sci. Technol.* **2002**, *174*, 151. (d) Ikeda, E.; Nicholls, P.; Mackie, J. C. *Proc. Comb. Inst.* **2000**, *28*, 1709. (e) Lifshitz, A.; Tamburu, C.; Suslensky, A. *J. Phys. Chem.* **1989**, *93*, 5802. (f) Mackie, J. C.; Colket, M. B., III; Nelson, P. F. *J. Phys. Chem.* **1990**, *94*, 4099. (g) MacNamara, J. P.; Simmie, J. M. *Comb. Flame* **2003**, *133*, 231.

(7) (a) Bacskay, G. B.; Martoprawiro, M.; Mackie, J. C. *Chem. Phys. Lett.* **1999**, *300*, 321. (b) Martoprawiro, M.; Bacskay, G. B.; Mackie, J. C. *J. Phys. Chem. A* **1999**, *103*, 3923. (c) Dubnikova, F.; Lifshitz, A. *J. Phys. Chem. A* **1998**, *102*, 10880.

(8) Kawaguchi, S.; Kumasaki, M.; Wada, Y.; Arai, M.; Tamura, M. *Kayaku Gakkaishi* **2001**, *62*, 16.

(9) (a) Lesnikovich, A. I.; Ivashkevich, O. A.; Lyutsko, V. A.; Printsev, G. V.; Kovalenko, K. K.; Gaponik, P. N.; Levchik, S. V. *Thermochim. Acta* **1989**, *145*, 195. (b) Vyazovkin, S. V.; Lesnikovich, A. I.; Lyutsko, V. A. *Thermochim. Acta* **1990**, *165*, 17.

(10) (a) Winnewisser, M.; Vogt, J.; Ahlbrecht, H. *J. Chem. Res. (S)* **1978**, 289. (b) Gilchrist, T. L.; Gymer, G. E.; Rees, C. W. *J. Chem. Soc., Perkin Trans. 1* **1975**, 1.

(11) Bock, H.; Dammel, R.; Aygen, S. *J. Am. Chem. Soc.* **1983**, *105*, 7681.

(12) (a) Gianola, A. J.; Ichino, T.; Hoenigman, R. L.; Kato, S.; Bierbaum, V. M.; Lineberger, W. C. *J. Phys. Chem. A* **2004**, *108*, 10326. (b) Gianola, A. J.; Ichino, T.; Hoenigman, R. L.; Kato, S.; Bierbaum, V. M.; Lineberger, W. C. *J. Phys. Chem. A* **2005**, *109*, 11504. (c) Gianola, A. J.; Ichino, T.; Kato, S.; Bierbaum, V. M.; Lineberger, W. C. *J. Phys. Chem. A* **2006**, *110*, 8457. (d) Gutowski, K. E.; Rogers, R. D.; Dixon, D. A. *J. Phys. Chem. A* **2006**, *110*, 11890. (e) Chen, Z. X.; Xiao, H. M.; Chiu, Y. N. *J. Phys. Chem. A* **1999**, *103*, 8062. (f) Alkorta, I.; Elguero, J. *Tetrahedron* **2006**, *62*, 8683. (g) Matus, M. H.; Arduengo, A. J., III; Dixon, D. A. *J. Phys. Chem. A* **2006**, *110*, 10116.

(13) (a) Dyke, J. M.; Groves, A. P.; Morris, A.; Ogden, J. S.; Dias, A. A.; Oliveira, A. M. S.; Costa, M. L.; Barros, M. T.; Cabral, M. H.; Moutinho, A. M. C. *J. Am. Chem. Soc.* **1997**, *119*, 6883. (b) Dyke, J. M.; Groves, A. P.; Morris, A.; Ogden, J. S.; Catarino, M. I.; Dias, A. A.; Oliveira, A. M. S.; Costa, M. L.; Barros, M. T.; Cabral, M. H.; Moutinho, A. M. C. *J. Phys. Chem. A* **1999**, *103*, 8239. (c) Dyke, J. M.; Levita, G.; Morris, A.; Ogden, J. S.; Dias, A. A.; Algarra, M.; Santos, J. P.; Costa, M. L.; Rodrigues, P.; Barros, M. T. *J. Phys. Chem. A* **2004**, *108*, 5299. (d) Hooper, N.; Beeching, L. J.; Dyke, J. M.; Morris, A.; Ogden, J. S.; Dias, A. A.; Costa, M. L.; Barros, M. T.; Cabral, M. H.; Moutinho, A. M. C. *J. Phys. Chem. A* **2002**, *106*, 9968.

Diels–Alder reactions (retro-[4 + 2]-cycloadditions), where in our mechanism we are producing a relatively unstable 1,2-diene, as opposed to a 1,3-diene. The tautomers formed by N to C hydrogen migration in the five-membered nitrogen heterocycles should also undergo similar cycloreversions, although these reactions are outside of the scope of this study, as they produce a different product set.

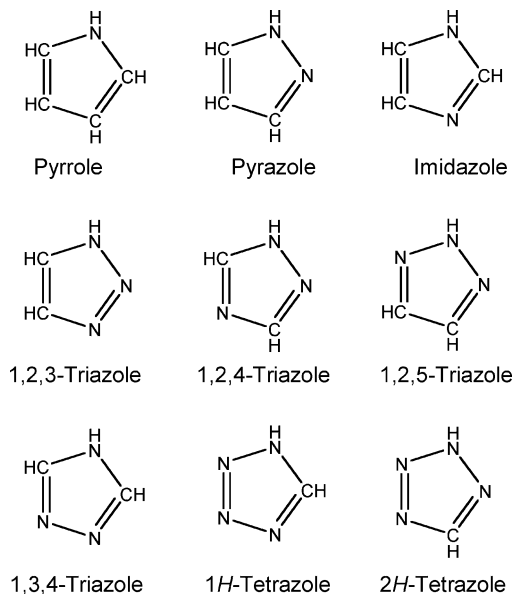
The dienes that we propose as dissociation products of the five-membered nitrogen-containing heterocycles are known to be of importance in numerous other reaction systems, and it is not uncommon for them to be detected as intermediates in matrix isolation studies. The species NHCCH_2 (ketenimine or ethenimine) has been recently detected in interstellar media.¹⁴ Ketenimine has also been identified as an intermediate in the decomposition of acetyl cyanide¹⁵ and 1-methylcytosine,¹⁶ a substituted six-membered nitrogen-containing heterocycle. HN_3 (hydrazoic acid or hydrogen azide) is of considerable atmospheric interest;¹⁷ hydrazoic acid is readily produced by the hydrolysis of sodium azide, which is the primary ingredient in automobile airbag inflation. Hydrazoic acid is known to readily photodissociate to $\text{N}_2 + \text{NH}$ and $\text{N}_3 + \text{H}$. Carbodiimides (NHCNH) are important intermediates in deamination of the nucleobase guanine,¹⁸ while carbodiimide has also been suggested as an intermediate in urea decomposition.¹⁹ Nitrilimine (diazenylmethylene, NHNCH) was reported to be a stable gas-phase molecule by Goldberg et al.²⁰ Nitrilimine and its derivatives are used in heterocyclic synthesis reactions, following a cycloaddition mechanism.²¹ According to their common occurrence as reaction intermediates, there is considerable value in determining the thermochemical properties of these dissociation products, irrespective of their role in the dissociation of their parent heterocycles.

In this contribution, we study the RCA reaction kinetics of nine five-membered nitrogen-containing heterocycles (depicted in Scheme 2) using theoretical methods. One goal is to identify if a retro-[3 + 2]-cycloaddition is an important first step in heterocycle decomposition, and if so, our calculations will provide important thermochemical and kinetic parameters for modeling the initial stages of heterocycle decomposition. Similar reactions may also prove to be of importance in the decomposition of six-membered nitrogen-containing heterocycles, or even cyclic compounds containing oxygen or other heteroatoms.

Computational Methods

Calculations are performed on all reactants, products, and transition states in the retro-[3 + 2]-cycloadditions of pyrrole, pyrazole, imidazole, 1,2,3-triazole, 1,2,4-triazole, 1,2,5-triazole, 1,3,4-triazole, 1*H*-tetrazole, and 2*H*-tetrazole, with the G3B3

SCHEME 2. Five-Membered Nitrogen-Containing Heterocycles Considered in This Study



composite theoretical method.²² For the parent heterocycles (excluding 1,2,4- and 1,3,4-triazole), we use G3B3 results reported in a previous study.⁴ In addition to the G3B3 calculations, the reaction products are treated with the high-level W1 composite theoretical method.²³ Results of the G3B3 and W1 calculations (geometries and enthalpies) are provided in the Supporting Information. All calculations were performed using Gaussian 03.²⁴ For all structures, including transition states, B3LYP/6-31G(d) geometries and frequencies were used to determine S°_{298} and $C_p(T)$ ($300 \text{ K} < T < 1500 \text{ K}$) using the SMCPS program,²⁵ and these values are found in the Supporting Information.

The G3B3 composite method involves an initial geometry optimization and frequency calculation at the B3LYP/6-31G(d) level. This is followed by various higher-level energy corrections to account for the theoretical method and the size of the basis set. The W1 method also uses B3LYP geometries and frequencies, but with the larger cc-pVTZ+d correlation-consistent basis set. The B3LYP geometry is then used in CCSD single-point energy calculations with correlation-consistent basis sets from double- through quadruple- ζ , extrapolated to the

(22) Baboul, A. G.; Curtiss, L. A.; Redfern, P. C.; Raghavachari, K. *J. Chem. Phys.* **1999**, *110*, 7650.

(23) Martin, J. M. L.; de Oliveira, G. *J. Chem. Phys.* **1999**, *111*, 1843.

(24) Frisch, M. J.; Trucks, G. W.; Schlegel, H. B.; Scuseria, G. E.; Robb, M. A.; Cheeseman, J. R.; Montgomery, J. A., Jr.; Vreven, T.; Kudin, K. N.; Burant, J. C.; Millam, J. M.; Iyengar, S. S.; Tomasi, J.; Barone, V.; Mennucci, B.; Cossi, M.; Scalmani, G.; Rega, N.; Petersson, G. A.; Nakatsuji, H.; Hada, M.; Ehara, M.; Toyota, K.; Fukuda, R.; Hasegawa, J.; Ishida, M.; Nakajima, T.; Honda, Y.; Kitao, O.; Nakai, H.; Klene, M.; Li, X.; Knox, J. E.; Hratchian, H. P.; Cross, J. B.; Adamo, C.; Jaramillo, J.; Gomperts, R.; Stratmann, R. E.; Yazyev, O.; Austin, A. J.; Cammi, R.; Pomelli, C.; Ochterski, J. W.; Ayala, P. Y.; Morokuma, K.; Voth, G. A.; Salvador, P.; Dannenberg, J. J.; Zakrzewski, V. G.; Dapprich, S.; Daniels, A. D.; Strain, M. C.; Farkas, O.; Malick, D. K.; Rabuck, A. D.; Raghavachari, K.; Foresman, J. B.; Ortiz, J. V.; Cui, Q.; Baboul, A. G.; Clifford, S.; Cioslowski, J.; Stefanov, B. B.; Liu, G.; Liashenko, A.; Piskorz, P.; Komaromi, I.; Martin, R. L.; Fox, D. J.; Keith, T.; Al-Laham, M. A.; Peng, C. Y.; Nanayakkara, A.; Challacombe, M.; Gill, P. M. W.; Johnson, B.; Chen, W.; Wong, M. W.; Gonzalez, C.; Pople, J. A. *Gaussian 03*, revision D.01; Gaussian, Inc.: Wallingford, CT, 2004.

(25) Sheng, C. Ph.D. Dissertation, New Jersey Institute of Technology, 2002.

(14) Lovas, F. J.; Hollis, J. M.; Remijan, A. J.; Jewell, P. R. *Astrophys. J.* **2006**, *645*, L137.

(15) Guennoun, Z.; Couturier-Tamburelli, I.; Combes, S.; Aycard, J. P.; Piétri, N. *J. Phys. Chem. A* **2005**, *109*, 11733.

(16) Yao, C.; Cuadrado-Peinado, M. L.; Poláček, M.; Tureček, F. *J. Mass Spectrom.* **2005**, *40*, 1417.

(17) Orlando, J. J.; Tyndall, G. S.; Berton, E. A.; Lowry, J.; Stegall, S. T. *Environ. Sci. Technol.* **2005**, *39*, 1632 and references therein.

(18) (a) Glaser, R.; Son, M.-S. *J. Am. Chem. Soc.* **1996**, *118*, 10942. (b) Glaser, R.; Rayat, S.; Lewis, M.; Son, M.-S.; Meyer, S. *J. Am. Chem. Soc.* **1999**, *121*, 6108.

(19) Tokmakov, I. V.; Alavi, S.; Thompson, D. L. *J. Phys. Chem. A* **2006**, *110*, 2759.

(20) Goldberg, N.; Fiedler, A.; Schwarz, H. *Helv. Chim. Acta* **1994**, *77*, 2354.

(21) For example, see: Mawhinney, R. C.; Muchall, H. M.; Peslherbe, G. H. *Can. J. Chem.* **2005**, *83*, 1615.

complete basis set limit. Corrections for core electron correlation and scalar relativistic effects are then applied to obtain the final W1 energy. The W1 method was found to provide a mean absolute error of $0.231 \text{ kcal mol}^{-1}$ for a test set of well-known atomization energies involving first-row elements. For a larger test set including first- and second-row atoms, the W1 method yields a maximum absolute error of $0.799 \text{ kcal mol}^{-1}$ and mean absolute error of $0.305 \text{ kcal mol}^{-1}$.²³ Comparatively, the G3B3 method provides an average absolute deviation of $0.99 \text{ kcal mol}^{-1}$ for the energies of the G2/97 test set.²²

Reaction rate parameters A' , n , and E_a were calculated for each dissociation reaction from transition state theory. Pre-exponential factors ($A(T)$) were calculated in the temperature range of 300 to 3000 K from $S^\circ(T)$. These values were then fit to A' and n , where $A = A'T^n$. High-pressure limit rate constants, $k^\infty(T)$, were calculated between 300 and 3000 K according to eq 1. Rate constants as a function of temperature and pressure ($k(T,P)$) were determined using the CHEMASTER program,²⁶ which describes falloff using the master equation. These calculations used an exponential-down energy transfer model ($\Delta E_{\text{down}} = 900 \text{ cal mol}^{-1}$), with estimated Lennard-Jones collision parameters $\sigma = 5 \text{ \AA}$ and $\epsilon/k = 550 \text{ K}^{-1}$, for all heterocycles. Stepwise reactions were treated using a multiple-well protocol in CHEMASTER, where the ring-opening product was considered as a chemically activated adduct, which could further dissociate to new reaction products, isomerize to the parent heterocycle, or be stabilized by collisions with the bath gas (N_2). Chemical activation was treated using quantum Rice–Ramsperger–Kassel (QRRK) theory, which approximates full RRKM theory using a reduced set of three representative vibrational frequencies.

$$k = A'T^n \exp\left(\frac{-E_a}{RT}\right) \quad (1)$$

Results and Discussion

Reaction Mechanism. As discussed in the Introduction, all of the studied dissociation reactions result in the formation of two-membered + three-membered products. When the three-membered product is $\text{NH}=\text{C}=\text{CH}_2$ or $\text{NH}=\text{C}=\text{NH}$, an intramolecular hydrogen shift reaction is required, and we discover that this hydrogen shift occurs in concert with the dissociation of either one or two bonds. Specifically, three reaction classes are identified:

(i) Simple Retro-[3 + 2]-Cycloaddition. These reactions involve two bond-breaking processes and lead to the three-membered products $\text{NH}=\text{N}=\text{CH}$ and $\text{NH}=\text{N}=\text{N}$. These reactions are involved in the dissociation of pyrazole, 1,2,4-, 1,2,3-, and 1,2,5-triazole and 2*H*- and 1*H*-tetrazole.

(ii) Retro-[3 + 2]-Cycloaddition with a Concerted Hydrogen Shift. Here, reaction involves the dissociation of two bonds and the migration of a H atom in the three-membered dissociation product from the central C atom to a terminal CH or N moiety. The three-membered dissociation products formed in these reactions are $\text{NH}=\text{C}=\text{CH}_2$ and $\text{NH}=\text{C}=\text{NH}$. This class of reactions is found in the dissociation of imidazole and 1,2,4- and 1,3,4-triazole. In Figure 1, we present an intrinsic reaction coordinate (IRC) scan for the decomposition of 1,2,4-triazole to $\text{NH}=\text{C}=\text{NH} + \text{HCN}$ and to $\text{NH}=\text{N}=\text{CH} + \text{HCN}$; the

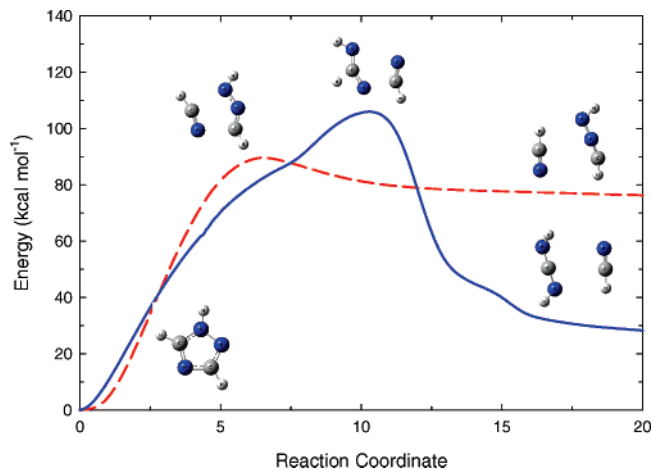


FIGURE 1. Intrinsic reaction coordinate scans for the decomposition of 1,2,4-triazole to $\text{NHCNH} + \text{HCN}$ (solid blue) and to $\text{NHNCH} + \text{HCN}$ (dashed red) at the B3LYP/6-31G(d) level.

reaction producing $\text{NH}=\text{C}=\text{NH}$ is class (ii) and involves an intramolecular hydrogen shift, with the other reaction being class (i). We observe that both reactions proceed via a concerted path between the reactant and the products, where the reaction to $\text{NH}=\text{N}=\text{CH} + \text{HCN}$ involves two bond-breaking processes, and the reaction to $\text{NH}=\text{C}=\text{NH} + \text{HCN}$ involves the dissociation of two bonds and an intramolecular hydrogen shift from a C to N site.

(iii) Ring Opening Followed by Dissociation with a Concerted Hydrogen Shift. This class of reactions follows a stepwise mechanism, with initial ring opening of the heterocycle (ring-chain tautomerism), followed by unimolecular bond dissociation leading to the dissociation products. In all cases, the bond dissociation reaction step exhibits a concerted hydrogen shift as for reactions (ii) above. This class of reactions produces the three-membered products $\text{NH}=\text{C}=\text{CH}_2$ and $\text{NH}=\text{C}=\text{NH}$ and is involved in the dissociation of pyrrole, pyrazole, 1,2,3-triazole, and 1*H*-tetrazole. The respective open-chain intermediates formed in the dissociation reactions of these four heterocycles are cyclopropane methanimine (*cyclo*- $\text{CH}=\text{CH}-\text{CH}(\text{CH}=\text{NH})$), 2*H*-azirine-2-methanimine (*cyclo*- $\text{CH}=\text{N}-\text{CH}(\text{CH}=\text{NH})$), diazoethanimine ($\text{NH}=\text{CH}-\text{CH}=\text{N}^+=\text{N}^-$), and methanimidoyl azide ($\text{NH}=\text{CH}-\text{N}=\text{N}^+=\text{N}^-$). In all cases, the open-chain tautomer is less stable than the parent heterocycle and is formed with a barrier below that for the second (dissociation) reaction step. In Figure 2, we provide a potential energy diagram for the 1*H*-tetrazole $\rightarrow \text{NH}=\text{C}=\text{NH} + \text{N}_2$ reaction, which is a representative class (iii) reaction. Figure 2 illustrates the energetics of each reaction step, as well as the bond-forming and -breaking processes occurring in the first and second transition states. Finally, we also note that in solution the zwitterionic intermediates that can be formed from ring opening of the heterocycles may be stabilized by medium effects. This could, in turn, lead to accelerated rates of heterocycle decomposition in solution.

Thermochemistry. Thermochemical parameters have been calculated for each of the RCA reaction products, using the G3B3 and W1 composite theoretical methods. Enthalpies of formation, calculated via atomization work reactions, are presented in Table 1 for both methods. With a composite theoretical method such as G3B3, the use of isodesmic work reactions is typically preferable to the atomization approach used here; isodesmic reactions feature the same number and type of

(26) Sheng, C.; Bozzelli, J. W.; Dean, A. M.; Chang, A. Y. *J. Phys. Chem. A* **2002**, *106*, 7276.

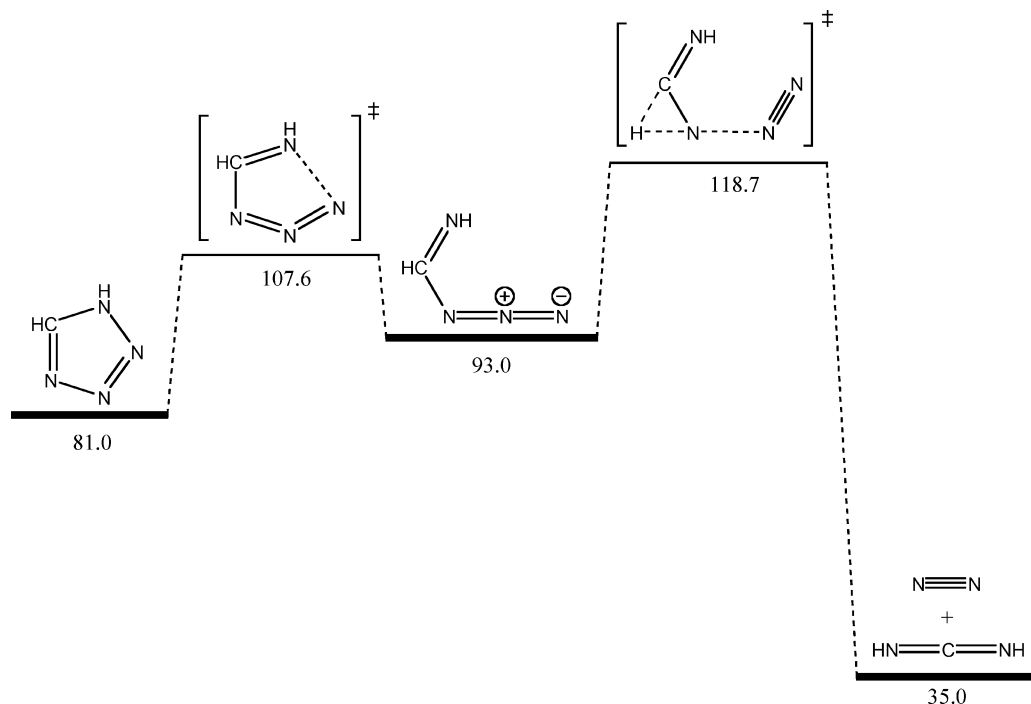


FIGURE 2. Potential energy diagram for the stepwise dissociation of 1*H*-tetrazole to $\text{NH}=\text{C}=\text{NH} + \text{N}_2$. Enthalpies of formation at 298 K, in kcal mol^{-1} .

TABLE 1. Calculated Enthalpies for the Dissociation Products of the Five-Membered Nitrogen-Containing Heterocycles^a

	$\Delta_f H^\circ_{298}$ (G3B3) ^b	$\Delta_f H^\circ_{298}$ (W1) ^b	$\Delta_f H^\circ_{298}$ (exptl)
HCCH	54.50	54.38	54.19 ²⁷
HCN	30.69	31.12	31.35 ²⁷
N_2	0.59	0.58	0.00
$\text{NH}=\text{C}=\text{CH}_2$	44.49	44.28	
$\text{NH}=\text{N}^+=\text{CH}^-$	88.30	88.75	
$\text{NH}=\text{N}^+=\text{N}^-$	70.00	70.09	
$\text{NH}=\text{C}=\text{NH}$	35.08	35.03	

^a All values in kcal mol^{-1} . ^b Calculated using atomization work reactions.

bonds on either side of the reaction and offer considerable error cancellation (in this instance, mean deviations would be reduced from ca. 1 down to around $0.5 \text{ kcal mol}^{-1}$).²⁸ However, with the accurate W1 method, where the average computational error is already around $0.5 \text{ kcal mol}^{-1}$, it is not clear that isodesmic work reactions would provide any significant increase in accuracy. Furthermore, da Silva et al.⁴ recently discussed how a lack of accurate reference enthalpies for nitrogen-containing compounds makes the application of isodesmic work reactions difficult when studying molecules such as these.

Where available, the calculated enthalpies presented in Table 1 are compared to literature values, and there is good agreement. The G3B3 and W1 enthalpies are also in excellent agreement, with an average difference of $0.19 \text{ kcal mol}^{-1}$ and maximum

(27) Chase, M. W., Jr. *J. Phys. Chem. Ref. Data, Monograph 9* **1998**, 1.

(28) (a) Raghavachari, K.; Stefanov, B. B.; Curtiss, L. A. *J. Chem. Phys.* **1997**, *106*, 6764. (b) da Silva, G.; Sebban, N.; Bozzelli, J. W.; Bockhorn, H. *ChemPhysChem* **2006**, *7*, 1119. (c) da Silva, G.; Chen, C.-C.; Bozzelli, J. W. *Chem. Phys. Lett.* **2006**, *424*, 42. (d) da Silva, G.; Kim, C.-H.; Bozzelli, J. W. *J. Phys. Chem. A* **2006**, *110*, 7925. (e) da Silva, G.; Bozzelli, J. W. *J. Phys. Chem. A* **2006**, *110*, 13058. (f) da Silva, G.; Bozzelli, J. W. *J. Phys. Chem. C* **2007**, *111*, 5760. (g) da Silva, G.; Chen, C.-C.; Bozzelli, J. W. *J. Phys. Chem. A* **2007**, *111*, 8663. (h) da Silva, G.; Bozzelli, J. W. *J. Phys. Chem. A* **2007**, *111*, 12026.

difference of $0.45 \text{ kcal mol}^{-1}$ (for NHNCH). This agreement supports our use of atomization work reactions. From our calculations, we recommend the W1 enthalpies of formation as the best available values for NHCCH₂, NHNCH, NHNN, and NHCNH. As outlined in the Introduction, these species are important intermediates in a variety of reaction processes. For nitrilimine, both theoretical methods predict a ground state geometry with *C*₁ point group symmetry, consistent with an allenic structure.²⁹

Reaction enthalpies and free energies (at 298 K) for each of the proposed dissociation reactions are listed in Table 2. The reaction enthalpies are calculated using literature enthalpies for the heterocycles (from ref 4) and either experimental or calculated W1 enthalpies for the dissociation products (cf. Table 1). For the heterocycles 1,2,5-triazole and 1,3,4-triazole, which were not studied in ref 4, and for the ring-opening products cyclopropane methanimine, 2*H*-azirine-2-methanimine, diazoethanimine, and methanimidoyl azide, we have calculated enthalpies of formation at the G3B3 level from atomization work reactions. Enthalpies of formation used for each of the heterocycles and their ring-opening products (where applicable) are listed in Table 3. Data in Table 2 illustrate a decreasing trend in enthalpy change for reaction to the products with increasing nitrogen content. The data also show that the most exothermic (or least endothermic) reactions are those involving N_2 production. Where a heterocycle shows decomposition pathways to both HCN and HCCH, we find that the reaction leading to HCN is always more energetically favorable.

The molecule pentazole (*cyclo*-N₅H) has been proposed as an energy-dense nitrogen-rich compound. While salts of the

(29) (a) Wong, M. W.; Wentrup, C. *J. Am. Chem. Soc.* **1993**, *115*, 7743. (b) Cargnoni, F.; Molteni, G.; Cooper, D. L.; Raimondi, M.; Ponti, A. *Chem. Commun.* **2006**, 1030. (c) Fauré, J.-L.; Réau, R.; Wong, M. W.; Koch, R.; Wentrup, C.; Bertrand, G. *J. Am. Chem. Soc.* **1997**, *119*, 2819. (d) Gronert, S.; Keeffe, J. R. *J. Org. Chem.* **2007**, *72*, 6343.

TABLE 2. Reaction Enthalpies and Free Energies for Dissociation of the Five-Membered Nitrogen-Containing Heterocycles^a

reaction	$\Delta_{\text{rxn}}H^\circ_{298}$ ^b	$\Delta_{\text{rxn}}G^\circ_{298}$ ^c
(1) pyrrole \rightarrow cyclopropane methanimine	64.30	61.69
(2) cyclopropane methanimine \rightarrow NH=C=CH ₂ + HCCH	7.67	-2.63
(3) pyrazole \rightarrow 2H-azirine-2-methanimine	45.60	43.93
(4) 2H-azirine-2-methanimine \rightarrow NH=C=CH ₂ + HCN	-12.37	-23.41
(5) pyrazole \rightarrow NH=N=CH + HCCH	100.54	88.17
(6) imidazole \rightarrow NH=C=CH ₂ + HCN	43.73	31.03
(7) imidazole \rightarrow NH=C=NH + HCCH	57.32	45.37
(8) 1,2,3-triazole \rightarrow NH=N=N + HCCH	60.58	48.45
(9) 1,2,3-triazole \rightarrow diazoethanimine	19.76	17.87
(10) diazoethanimine \rightarrow NH=C=CH ₂ + N ₂	-39.18	-49.46
(11) 1,2,4-triazole \rightarrow NH=C=NH + HCN	19.58	7.45
(12) 1,2,4-triazole \rightarrow NH=N=CH + HCN	73.38	60.77
(13) 1,2,5-triazole \rightarrow NH=N=CH + HCN	59.94	47.00
(14) 1,3,4-triazole \rightarrow NH=C=NH + HCN	13.80	1.33
(15) 1H-tetrazole \rightarrow NH=N=N + HCN	20.44	8.21
(16) 1H-tetrazole \rightarrow methanimidoyl azide	11.98	10.41
(17) methanimidoyl azide \rightarrow NH=C=NH + N ₂	-57.95	-67.91
(18) 2H-tetrazole \rightarrow NH=N=CH + N ₂	9.75	-2.24
(19) 2H-tetrazole \rightarrow NH=N=N + HCN	22.44	10.16

^a All values in kcal mol⁻¹. ^b Calculated from literature, WI, and G3B3 enthalpies of formation. ^c Calculated from $\Delta_{\text{rxn}}H^\circ_{298}$ using B3LYP/6-31G(d) entropies.

TABLE 3. Enthalpies of Formation of the Five-Membered Nitrogen Heterocycles and Their Relevant Open-Chain Tautomers

	$\Delta_f H^\circ_{298}$	source
pyrrole	26.5	4
pyrazole	42.4	4
imidazole	31.9	4
1,2,3-triazole	63.7	4
1,2,4-triazole	46.8	4
1,2,5-triazole	60.16	G3B3
1,3,4-triazole	52.58	G3B3
1H-tetrazole	81.0	4
2H-tetrazole	79.0	4
cyclopropane methanimine	90.80	G3B3
2H-azirine-2-methanimine	88.00	G3B3
diazoethanimine	83.46	G3B3
methanimidoyl azide	92.98	G3B3

pentazolide ion (*cyclo*-N₅⁻) have been reported,¹ to our knowledge, the pentazole molecule remains to be successfully synthesized. If it exists, pentazole should undergo a retro-[3 + 2]-cycloaddition to N₂ + NH=N=N. The enthalpy and free energy (298 K) of formation of pentazole were calculated as 108.9 and 89.9 kcal mol⁻¹ by da Silva et al.⁴ using the CBS-APNO theoretical method (298 K entropy = 63.15 cal mol⁻¹ K⁻¹). Using our calculated enthalpy of formation for NHNN and 298 K entropies for NHNN and N₂, we find the retro-cycloaddition of pentazole to be exothermic by 38.8 kcal mol⁻¹, with a free energy of reaction of -50.7 kcal mol⁻¹ at 298 K. This high exothermicity should result in a small barrier for dissociation.

Dissociation Kinetics. Transition states have been located for each of the proposed dissociation reactions, and they are illustrated in the Supporting Information. The reactions dissociating to NH=C=NH and NH=C=CH₂ are those exhibiting an intramolecular hydrogen shift (reactions 2, 4, 6, 7, 10, 11, 14, and 17). As mentioned in the Introduction, this is due to the high reactivity (instability) of the N•H-CH=C•H and N•H-CH=N• diradicals. The effect of this concerted hydrogen transfer process occurring in the transition state on the dissociation kinetics is examined later.

Activation enthalpies and activation free energies (at 298 K) are presented in Table 4 for each of the studied reactions. As with the reaction enthalpies, we again notice a general trend

TABLE 4. Activation Enthalpies (ΔH^\ddagger_{298}) and Activation Free Energies (ΔG^\ddagger_{298}) for RCA Reactions of the Five-Membered Nitrogen-Containing Heterocycles^a

reaction	ΔH^\ddagger_{298}	ΔG^\ddagger_{298}
(1 _f) pyrrole \rightarrow cyclopropane methanimine	98.26	96.90
(1 _r) cyclopropane methanimine \rightarrow pyrrole	33.96	35.21
(2) cyclopropane methanimine \rightarrow NH=C=CH ₂ + HCCH	71.60	69.39
(3 _f) pyrazole \rightarrow 2H-azirine-2-methanimine	78.22	77.14
(3 _r) 2H-azirine-2-methanimine \rightarrow pyrazole	32.62	33.21
(4) 2H-azirine-2-methanimine \rightarrow NH=C=CH ₂ + HCN	54.06	51.85
(5) pyrazole \rightarrow NH=N=CH + HCCH	108.15	105.54
(6) imidazole \rightarrow NH=C=CH ₂ + HCN	104.82	101.15
(7) imidazole \rightarrow NH=C=NH + HCCH	124.06	120.61
(8) 1,2,3-triazole \rightarrow NH=N=N + HCCH	81.18	79.14
(9 _f) 1,2,3-triazole \rightarrow diazoethanimine	27.57	27.07
(9 _r) diazoethanimine \rightarrow 1,2,3-triazole	7.81	9.20
(10) diazoethanimine \rightarrow NH=C=CH ₂ + N ₂	31.96	30.21
(11) 1,2,4-triazole \rightarrow NH=C=NH + HCN	96.55	93.32
(12) 1,2,4-triazole \rightarrow NH=N=CH + HCN	82.09	80.06
(13) 1,2,5-triazole \rightarrow NH=N=CH + HCN	72.58	70.11
(14) 1,3,4-triazole \rightarrow NH=C=NH + HCN	82.57	79.65
(15) 1H-tetrazole \rightarrow NH=N=N + HCN	46.51	45.00
(16 _f) 1H-tetrazole \rightarrow methanimidoyl azide	26.57	26.21
(16 _r) methanimidoyl azide \rightarrow 1H-tetrazole	14.59	15.79
(17) methanimidoyl azide \rightarrow NH=C=NH + N ₂	25.68	25.25
(18) 2H-tetrazole \rightarrow NH=N=CH + N ₂	37.82	36.37
(19) 2H-tetrazole \rightarrow NH=N=N + HCN	54.51	53.18

^a Calculated at the G3B3 level. All values in kcal mol⁻¹.

corresponding to decreasing enthalpy with increasing nitrogen content. It is well-known that the energies (free energy or enthalpy) of activation and reaction, within a class of similar reactions, are often inter-related, and correlations can be developed between the two parameters. We have attempted such a correlation with the reaction and activation enthalpies, according to a variable-order form of the Marcus equation.

The intrinsic barrier for a series of related reactions which proceed via a similar mechanism can be calculated by fitting the Marcus equation to a plot of the free energy of reaction versus the free energy of activation, provided that the intrinsic barrier does not change due to a shift in reaction mechanism. We propose a modified variable-order form of the Marcus equation, given by eq 2. Here, ΔG° is the free energy of reaction,

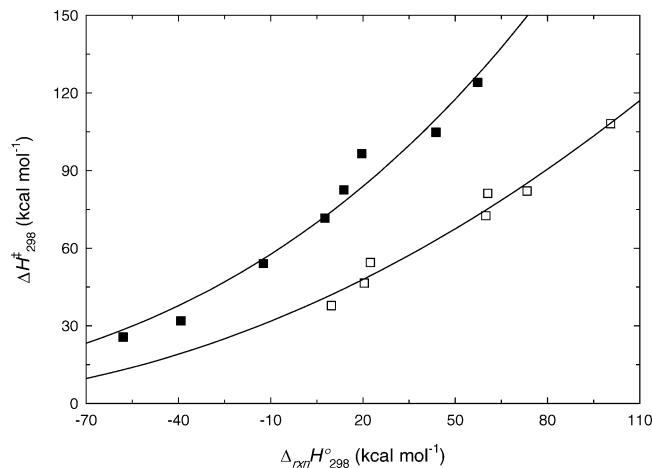


FIGURE 3. Relationship between reaction enthalpy and activation enthalpy for heterocycle dissociation with (■) and without (□) an intramolecular hydrogen shift. Solid lines indicate fits of the Marcus equation (described in the text).

ΔG^\ddagger is the free energy of activation, ΔG_o^\ddagger is the intrinsic barrier to reaction, and n is the variable-order exponent introduced here.³⁰ The classical form of the Marcus equation is quadratic, with $n = 2$.³⁰ In our following analysis, we will apply eq 2 to enthalpies (ΔH°_{298} versus ΔH^\ddagger_{298}) instead of free energies. However, similar relationships are developed with free energy (at 298 K), and these are provided as Supporting Information. The applicability of eq 2 to both enthalpies and free energies indicates that the entropy of reaction/activation is relatively constant within the studied series of reactions, and/or that there is a significant degree of enthalpy–entropy compensation.

$$\Delta G^\ddagger = \Delta G_o^\ddagger \left(1 + \frac{\Delta G^\circ}{4\Delta G_o^\ddagger} \right)^n \quad (2)$$

Upon plotting ΔH°_{298} versus ΔH^\ddagger_{298} , we observe that the data fall upon two distinct relationships: one for simple retro-[3 + 2]-cycloaddition (class (i)) and one for dissociation with an intramolecular hydrogen shift (class (ii) and class (iii)). The two separate reaction series were fit to eq 2 through an iterative least-squares error minimization technique, in which the intrinsic barrier (ΔH_o^\ddagger) and n were both varied; such a scheme has previously proven successful at simultaneously determining the intrinsic barrier to reaction and the free energy of reaction when using $n = 2$.³¹ Good fits of the calculated data were obtained using $\Delta H_o^\ddagger = 36.8 \text{ kcal mol}^{-1}$ and $n = 2.07$ for the simple RCA reactions (class (i)) and $\Delta H_o^\ddagger = 65.6 \text{ kcal mol}^{-1}$ and $n = 3.34$ for dissociation with the added hydrogen shift (class (ii) and class (iii)). The results for both reaction series are plotted in Figure 2. Similar relationships were obtained with reaction free energies and activation free energies, with intrinsic barriers of $\Delta G_o^\ddagger = 42.1$ and $73.1 \text{ kcal mol}^{-1}$ for the respective reaction series. These plots are provided as Supporting Information.

In Figure 3, we see that, for the same reaction enthalpy, the reactions involving an intramolecular hydrogen shift possess significantly higher barriers to reaction. This is manifested in the results of the Marcus equation analysis, where the intrinsic barrier to reaction is ca. 30 kcal mol^{-1} greater when the

transition state involves an intramolecular hydrogen shift. This result is not unexpected; according to the principle of nonperfect synchronization, the additional process occurring at the transition state would result in a loss of transition state synchronicity, which would increase the intrinsic barrier.³² In this context, the values of n obtained with the two reaction series are also interesting. For the simple RCA reactions, we find $n = 2.07$, which is close to the classical value of 2. However, for the open-shell products undergoing a concerted hydrogen shift to closed-shell systems, we find $n = 3.34$, which deviates significantly from the classical n value. It could be that such relationships between reaction energies and activation energies begin to deviate from the quadratic form of the classical Marcus equation with increasing loss of synchronicity in the transition state. By corollary, the degree to which n deviates from a value of 2 may provide some measure of transition state synchronicity, or lack thereof.

The main usefulness of correlations such as the above is suggesting possible fundamental concepts related to mechanism and energy needs; however, they also hold some predictive large errors (cf. Figure 2). As discussed earlier, the retro-[3 + 2]-cycloaddition of pentazole is more exothermic than any of the other dissociation reactions studied here. Extrapolating our Marcus equation relationship, we estimate that the dissociation of pentazole to $\text{N}_2 + \text{NHNN}$ will proceed with an activation enthalpy of only $19.5 \text{ kcal mol}^{-1}$ and free energy of activation of $19.2 \text{ kcal mol}^{-1}$ at 298 K. Such a low barrier makes it unlikely that pentazole would exist as a stable compound at standard temperature and pressure conditions. From the free energy of activation (and accounting for a reaction degeneracy of 2), canonical transition state theory provides a rate constant for pentazole decomposition of 0.10 s^{-1} at 298 K, corresponding to a half-life of 6.9 s. However, it is important to remember that this analysis neglects the effect of the heat generated by this exothermic reaction, which would result in an autocatalytic temperature increase in an adiabatic system. The significant uncertainty in this analysis, resulting from extrapolation of the Marcus equation relationship, should also be considered. However, Benin et al.³³ calculated the half-life of pentazole to be ca. 10 min at 0°C , whereas we calculate a value of ca. 2.4 min at this temperature. The respective calculations agree to within an order of magnitude (the calculations of Benin et al.³³ feature methanol as a solvent, while our calculations are performed in vacuo).

The pre-exponential rate parameters A' and n for the dissociation reactions were determined from the temperature dependence of $k(T)$, with E_a was set equal to ΔH^\ddagger_{298} . Fitted values of A' and n are presented in Table 5. Using the calculated rate parameters, we can determine $k(T,P)$ from a time-dependent solution of the master equation (QRRK/ME for the multiple-well reactions). These values are plotted in Figure 4 for each of the dissociation reactions at $P = 1 \text{ atm}$. For pyrrole and for 1,2,5- and 1,3,4-triazole dissociation, we have plotted $2k$ in Figure 4, so as to account for the two degenerate dissociation pathways available to these heterocycles. Rate constants as a function of T and P are listed in the Supporting Information.³⁴

From Figure 4, we find that the most rapid RCA reactions are the three reactions leading to N_2 formation. These reactions,

(30) (a) Marcus, R. A. *J. Chem. Phys.* **1956**, *24*, 966. (b) Marcus, R. A. *J. Phys. Chem.* **1968**, *72*, 891.

(31) da Silva, G.; Kennedy, E. M.; Dlugogorski, B. Z. *J. Phys. Org. Chem.* **2007**, *20*, 167.

(32) (a) Bernasconi, C. F. *Acc. Chem. Res.* **1992**, *25*, 9. (b) Bernasconi, C. F. *Tetrahedron* **1985**, *41*, 3219.

(33) Benin, V.; Kaszynski, P.; Radziszewski, J. G. *J. Org. Chem.* **2002**, *67*, 1354.

TABLE 5. Reaction Rate Parameters A' and n for Dissociation of the Five-Membered Nitrogen-Containing Heterocycles

reaction	A' (s^{-1})	n
(1 _p) pyrrole \rightarrow cyclopropane methanimine	1.35×10^{12}	0.71
(1 _r) cyclopropane methanimine \rightarrow pyrrole	2.21×10^{11}	0.22
(2) cyclopropane-methanimine \rightarrow NH=C=CH ₂ + HCCH	4.88×10^{10}	1.59
(3 _p) pyrazole \rightarrow 2H-azirine-2-methanimine	2.68×10^{11}	0.94
(3 _r) 2H-azirine-2-methanimine \rightarrow pyrazole	8.91×10^{11}	0.20
(4) 2H-azirine-2-methanimine \rightarrow NH=C=CH ₂ + HCN	8.44×10^{11}	1.08
(5) pyrazole \rightarrow NH=N=CH + HCCH	1.09×10^{11}	1.61
(6) imidazole \rightarrow NH=C=CH ₂ + HCN	3.14×10^{11}	1.73
(7) imidazole \rightarrow NH=C=NH + HCCH	2.17×10^{11}	1.78
(8) 1,2,3-triazole \rightarrow NH=N=N + HCCH	6.33×10^{11}	1.15
(9 _p) 1,2,3-triazole \rightarrow diazoethanimine	5.69×10^{11}	0.62
(9 _r) diazoethanimine \rightarrow 1,2,3-triazole	2.31×10^{11}	0.15
(10) diazoethanimine \rightarrow NH=C=CH ₂ + N ₂	4.26×10^{11}	1.02
(11) 1,2,4-triazole \rightarrow NH=C=NH + HCN	4.86×10^{11}	1.57
(12) 1,2,4-triazole \rightarrow NH=N=CH + HCN	3.55×10^{11}	1.25
(13) 1,2,5-triazole \rightarrow NH=N=CH + HCN	2.71×10^{11}	1.38
(14) 1,3,4-triazole \rightarrow NH=C=NH + HCN	8.91×10^{10}	1.71
(15) 1H-tetrazole \rightarrow NH=N=N + HCN	1.39×10^{12}	0.82
(16 _p) 1H-tetrazole \rightarrow methanimidoyl azide	1.71×10^{12}	0.37
(16 _r) methanimidoyl azide \rightarrow 1H-tetrazole	5.06×10^{11}	0.07
(17) methanimidoyl azide \rightarrow NH=C=NH + N ₂	7.49×10^{10}	0.95
(18) 2H-tetrazole \rightarrow NH=N=CH + N ₂	8.00×10^{11}	0.90
(19) 2H-tetrazole \rightarrow NH=N=N + HCN	6.07×10^{11}	0.92

which correspond to dissociation of 1H-tetrazole, 2H-tetrazole, and 1,2,3-triazole, should be rapid at high to moderate temperatures, and we suggest that these reactions will constitute the dominant reaction pathways in the initial decomposition of these heterocycles in thermal systems. The other decomposition pathway for 1,2,3-triazole should not be important, although the reactions leading to HCN + NHNN from both 1H- and 2H-tetrazole show relatively high rate constants and may constitute a secondary reaction pathway in the thermal reactions of these heterocycles. None of the other heterocycles exhibit rapid dissociation kinetics according to a retro-[3 + 2]-cycloaddition mechanism, and we expect that these reaction processes will be unimportant at all but high temperatures.

Comparison to Experiment. In this section, we attempt to correlate the results of our study with the results of experimental studies on the decomposition of five-membered nitrogen heterocycles, in terms of both reaction kinetics and the products formed.

Pyrrole. Pyrrole decomposes with an experimental activation energy of around 74 kcal mol⁻¹.^{6a,b} This is significantly lower than the barrier determined here for dissociation to NHCCH₂ + HCCH (ca. 140 kcal mol⁻¹), and we therefore conclude that the RCA mechanism is unimportant. Theoretical studies suggest that pyrrole decomposition proceeds via an initial 4,5-H shift, producing a cyclic carbene intermediate which ring opens and then dissociates to HCN + propyne. The initial H migration represents the rate-limiting step in this mechanism, with activation energy calculated as 75.6 kcal mol⁻¹.^{7a} The agreement between the theoretical and experimental activation energies provides support for the previously proposed mechanism. Also, we can rule out initial ring opening in pyrrole to cyclopropane methanimine as an important reaction process, due to the high barrier for reaction (98 kcal mol⁻¹).

(34) The master equation analysis shows that falloff becomes important at low pressures and high temperatures. For the faster dissociation reactions, falloff at moderate to high temperatures is still significant for atmospheric and greater pressures.

Pyrazole and Imidazole. The two-nitrogen atom heterocycles pyrazole and imidazole decompose via the proposed RCA mechanism with large barriers to reaction. For pyrazole, the total rate constant is calculated as $k [s^{-1}] = 1.87 \times 10^{17} \exp(-51900/T)$, and for imidazole, it is $k [s^{-1}] = 2.10 \times 10^{16} \exp(-53000/T)$ (both at 300–2000 K, 1 atm). These rate expressions correspond to respective activation energies of 103.0 and 105.3 kcal mol⁻¹. In pyrazole and imidazole, N–H bond dissociation energies have been calculated as 112.1 and 97.2 kcal mol⁻¹,⁴ respectively, and we would therefore expect N–H bond dissociation to be more important than the RCA reactions in imidazole pyrolysis. It is likely, however, that even lower energy reaction pathways are available to both heterocycles in both pyrolysis and combustion environments. For instance, ring opening of pyrazole to 2H-azirine-2-methanimine proceeds with a barrier of 78 kcal mol⁻¹.

Relatively little experimental information is available on the thermal decomposition of pyrazole and imidazole. The decomposition temperature of imidazole is quoted as 620–650 °C,³⁵ which is far too low for the proposed mechanism to be of importance (at 650 °C, the calculated RCA half-life of imidazole is 3×10^8 s). From flash vacuum pyrolysis experiments on pyrazole, the Arrhenius parameters $E_a = 71.3$ kcal mol⁻¹ and $A = 2.75 \times 10^{15} s^{-1}$ have been measured,³⁶ whereas we find values of 103.0 kcal mol⁻¹ and $1.87 \times 10^{15} s^{-1}$, again suggesting that the proposed RCA mechanism is not of importance. However, the initial ring-opening reaction to 2H-azirine-2-methanimine, with 298 K activation enthalpy of 78.22 kcal mol⁻¹, might be of some importance if followed by lower-barrier dissociation reactions.

Triazoles. From our calculated rate constants, 1,2,3-triazole exhibits the most rapid RCA decomposition kinetics of the triazoles studied, where stepwise decomposition to N₂ + NHCCH₂ yields a rate expression of $k [s^{-1}] = 4.40 \times 10^{16} \exp(-26700/T)$ at 300–1000 K and 1 atm, with an activation energy of 53.0 kcal mol⁻¹. Across the studied temperature and pressure range, neither the 1,2,3-triazole \rightarrow HCCH + NHNN reaction nor the 1,2,5-triazole \rightarrow HCN + NHNCH reaction was found to be important (at best, 1,2,5-triazole decomposition contributed 0.3% of the total reaction rate at 3000 K and 1000 atm). This analysis, however, neglects that 1,2,5-triazole is more stable than 1,2,3-triazole (by ca. 3.5 kcal mol⁻¹), where the equilibrium will lie toward the less reactive tautomer, effectively slowing the decomposition kinetics at temperatures where tautomerisation equilibrium is achieved.

Malow et al.³⁷ used differential scanning calorimetry (DSC) to examine 1,2,3-triazole decomposition, where the onset temperature for decomposition was found to be 599 K, with peak heat flow at 627 K (heating rate: 3–5 K min⁻¹). At these respective temperatures, we calculate half-lives of only 360 and 49 s. Given these results, we suggest that the proposed RCA reaction is the dominant mechanism in the thermal decomposition of 1,2,3-triazole. It should be noted that Katritzky et al.³⁸ also studied the thermal decomposition of 1,2,3-triazole using DSC and found that decomposition occurred in the much lower temperature range of 491–611 K (heating rate: 10 K min⁻¹).

(35) Johns, I. B.; McEhill, E. A.; Smith, J. O. *J. Chem. Eng. Data* **1962**, *7*, 277.

(36) Pérez, J. D.; Yranzo, G. I. *Bull. Soc. Chim. Fr.* **1985**, 473.

(37) Malow, M.; Wehrstedt, K. D.; Neuenfeld, S. *Tetrahedron Lett.* **2007**, *48*, 1233.

(38) Katritzky, A. R.; Wang, Z.; Tsikolia, M.; Hall, C. D.; Carman, M. *Tetrahedron Lett.* **2006**, *47*, 7653.

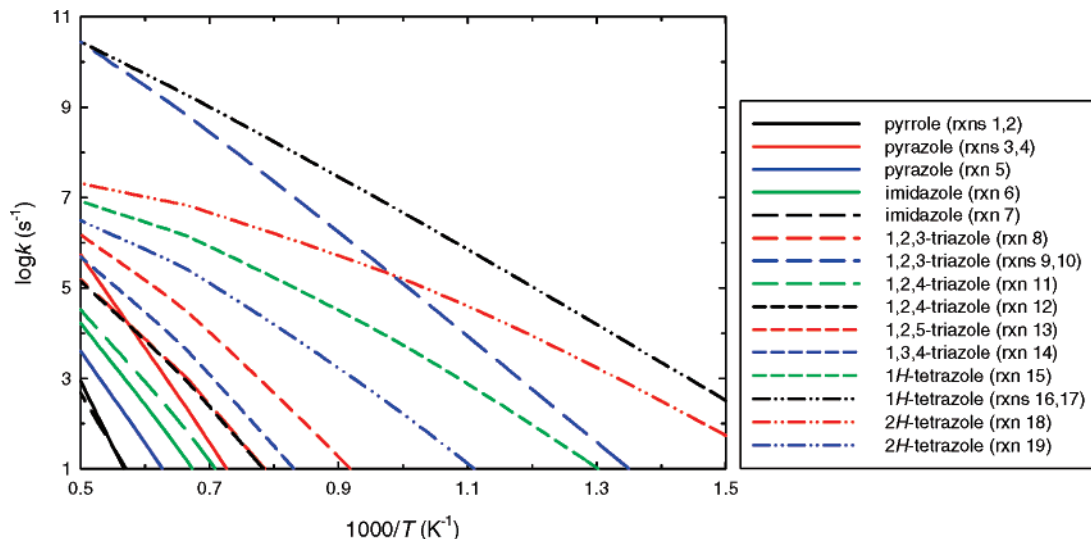


FIGURE 4. Rate constants ($k(T)$, s^{-1}) for dissociation of the five-membered nitrogen-containing heterocycles; $P = 1$ atm.

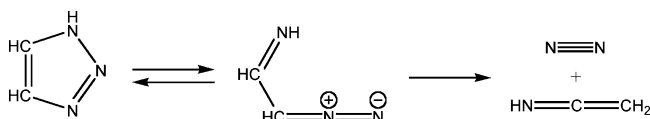


FIGURE 5. Retro-[3 + 2]-cycloaddition mechanism for 1,2,3-triazole decomposition.

From our calculated rate expression, we find a half-life of 6.5×10^6 s at 491 K and 150 s at 611 K. However, Malow et al.³⁷ point out a methodological flaw in the experiments of Katritzky et al.,³⁸ and we show later that their measured heat release is also far too small given the known products ($\text{CH}_3\text{CN} + \text{N}_2$) of 1,2,3-triazole decomposition.

For the dissociation of 1,2,3-triazole, we predict that ketenimine will be an important reaction intermediate. In thermal systems, ketenimine will isomerize to methyl isocyanide ($\text{CH}_3\text{-NC}$) and again to acetonitrile (CH_3CN).³⁹ This would explain the experimental observation of acetonitrile as the major decomposition product of 1,2,3-triazole pyrolysis.^{10,11} Acetonitrile produced during combustion is known to be a significant atmospheric pollutant.⁴⁰ In the DSC experiments of Katritzky et al., the decomposition of 1,2,3-triazole was found to be exothermic by only $2.1 \text{ kcal mol}^{-1}$ (126 J g^{-1}), while Malow et al.³⁷ measured the process to be $42.8 \text{ kcal mol}^{-1}$ exothermic (2600 J g^{-1}). We calculate the overall reaction $1,2,3\text{-triazole} \rightarrow \text{CH}_3\text{CN} + \text{N}_2$ to be $46.0 \text{ kcal mol}^{-1}$ exothermic (using an enthalpy of formation of $17.7 \text{ kcal mol}^{-1}$ for CH_3CN);⁴¹ our thermochemical data support the Malow et al.³⁷ DSC experiments. The suggested mechanism for 1,2,3-triazole decomposition is provided in Figure 5. This is a class (iii) reaction, according to our definitions.

For 1,2,4-triazole and its 7 kcal mol^{-1} less stable tautomer 1,3,4-triazole, we calculate total rate expressions for RCA decomposition of $k [s^{-1}] = 7.37 \times 10^{14} \exp(-36100/T)$ and $6.07 \times 10^{15} \exp(-41400/T)$, respectively, at 300–2000 K and

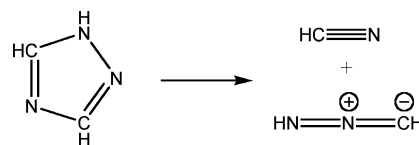


FIGURE 6. Retro-[3 + 2]-cycloaddition mechanism for 1,2,4-triazole decomposition. This proposed RCA mechanism may only constitute a minor reaction pathway.

1 atm ($E_a = 71.8$ and $82.2 \text{ kcal mol}^{-1}$). For 1,2,4-triazole, the reaction to $\text{NHNCH} + \text{HCN}$ dominates, with the $\text{NHCNH} + \text{HCN}$ reaction contributing up to 10% of the total reaction rate at 2000 K. The 1,3,4-triazole RCA reaction should always be insignificant, due to the greater barrier for reaction and the lower equilibrium concentration of the 1,3,4-triazole tautomer.

Kumasaki et al.⁴² studied the flash pyrolysis of 1,2,4-triazole and found that the overall reaction produced HCN and NH_3 at lower temperatures and HCN and CH_4 at higher temperatures. Kumasaki et al. proposed a similar decomposition mechanism to that studied here, based upon the results of theoretical calculations. It was suggested that at higher temperatures HCN and CH_4 could be formed via initial dissociation to $\text{HCN} + \text{nitrilimine (NHNCH)}$, with nitrilimine subsequently eliminating N_2 to yield CH_2 (which would abstract two H atoms to give CH_4). Experimentally, the decomposition mechanism leading to $\text{HCN} + \text{CH}_4$ was found to become important at around 600–700 °C, and in this temperature range, our calculated rate expression returns 1,2,4-triazole half-lives of 860 and 12 s, respectively. It is therefore plausible that the proposed mechanism contributes to 1,2,4-triazole decomposition, especially at higher temperatures. This mechanism is depicted in Figure 6, and we note that this is a class (i) RCA reaction.

Tetrazole. 1*H*-Tetrazole and 2*H*-tetrazole will tautomerize in thermal environments, and reactions 15–19 are therefore relevant to the thermal decomposition of both 1*H*- and 2*H*-tetrazole (hereafter referred to only as tetrazole). We calculate the total rate of tetrazole decomposition (the sum of the four reaction channels) as $k [s^{-1}] = 6.16 \times 10^{14} \exp(-19000/T)$ at

(39) (a) Doughty, A.; Bacskay, G. B.; Mackie, J. C. *J. Phys. Chem.* **1994**, *98*, 13546. (b) Yang, X.; Maeda, S.; Ohno, K. *J. Phys. Chem. A* **2005**, *109*, 7319.

(40) Brasseur, G.; Arijs, E.; De Rudder, A.; Nevejans, D.; Ingels, J. *Geophys. Res. Lett.* **1983**, *10*, 725.

(41) An, X.; Mansson, M. *J. Chem. Thermodyn.* **1983**, *15*, 287.

(42) Kumasaki, M.; Wada, Y.; Akutsu, Y.; Arai, M.; Tamura, M. *Kayaku Gakkaishi* **2001**, *62*, 147.

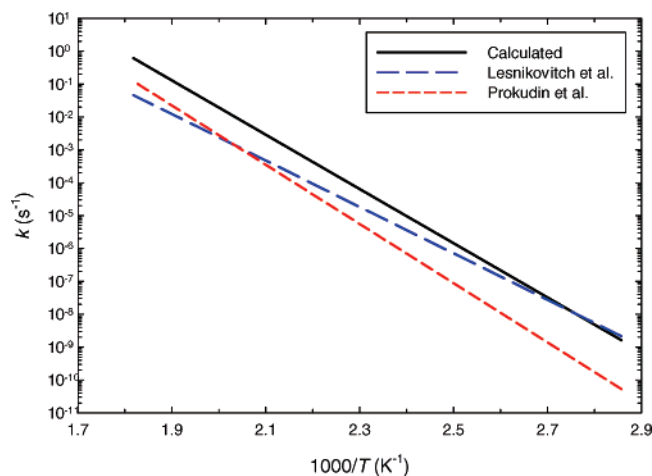


FIGURE 7. Comparison between calculated and experimental rate expressions for tetrazole pyrolysis.

300–2000 K and 1 atm. This corresponds to an activation energy of $37.8 \text{ kcal mol}^{-1}$. Of the four studied decomposition pathways, branching ratio analysis reveals that the $1H$ -tetrazole $\rightarrow \text{NHCNH} + \text{N}_2$ reaction dominates, with a significant contribution from the $2H$ -tetrazole $\rightarrow \text{NHNCH} + \text{N}_2$ reaction at low temperature and pressure conditions. This analysis assumes an equal equilibrium population of the two tautomers, which is a relatively valid assumption given their similar enthalpies of formation.

The thermal decomposition of tetrazole was studied using differential scanning calorimetry (DSC), differential automatic gas volumetry (DAGV), and complex thermal analysis by Lesnikovitch et al.^{9a} Tetrazole was found to decompose at temperatures of around 430 K and above. Thermogravimetric results were used to obtain the invariant kinetic parameters $E_a = 41.2 \text{ kcal mol}^{-1}$ and $A = 2.95 \times 10^{15} \text{ s}^{-1}$. The thermal decomposition of tetrazole was also studied by Prokudin et al.,⁴³ who obtained $E_a = 32.3 \pm 1.4 \text{ kcal mol}^{-1}$ and $A = 3.16 \times 10^{11} \text{ s}^{-1}$ in the temperature range of 453–503 K. The rate parameters determined in these two experimental studies compare well with our calculated values (excluding the A value of ref 43). This confirms that the RCA reaction identified in this study is the dominant reaction channel in the thermal decomposition of tetrazole. The calculated rate expression for tetrazole decomposition obtained in this study is compared in Figure 7 to these two experimental measurements, extrapolated over the temperature range of 350–550 K, where we find good agreement. The retro-[3 + 2]-cycloaddition mechanism for tetrazole decomposition identified in this study is illustrated in Figure 8, where the $1H$ -tetrazole pathway constitutes a class (iii) reaction and the $2H$ -tetrazole pathway constitutes a class (i) reaction.

The important intermediates in tetrazole decomposition will include carbodiimide, nitrilimine, hydrazoic acid, and hydrogen cyanide. Hydrazoic acid has been detected as the major stable decomposition product of tetrazole decomposition, while other important products included methane, ammonia, and ethene.⁸ Nitrilimine and carbodiimide were not reported, which suggests that these compounds are unstable intermediates, which react further (either unimolecularly, via abstraction reactions, or in

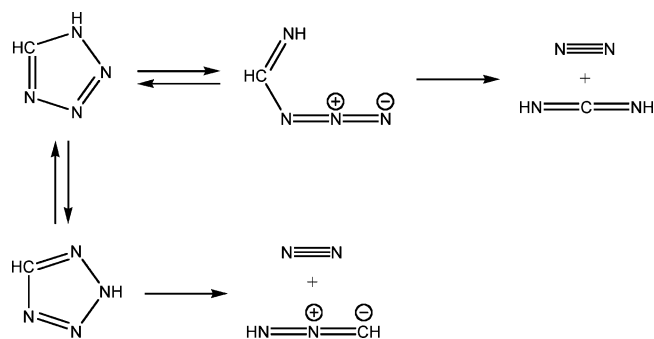


FIGURE 8. Retro-[3 + 2]-cycloaddition mechanism for $1H$ - and $2H$ -tetrazole decomposition.

chemically activated association or addition reactions with other species) to produce the experimentally observed reaction products. First, we would expect nitrilimine to rearrange to yield the more stable carbodiimide, with reaction enthalpy of $-53.22 \text{ kcal mol}^{-1}$ (other more stable isomers may also exist on the CN_2H_2 potential energy surface). Otherwise, nitrilimine might eliminate N_2 , forming CH_2 (methylene) in a reaction that is ca. 14 kcal mol^{-1} endothermic (to singlet methylene). In a less probable elimination reaction, the amino and cyano radicals are formed (ca. 61 kcal mol^{-1} endothermic). Nitrilimine could also dissociate to $\text{HN}_2 + \text{CH}$ (methylidyne). Species from the active radical pool would abstract hydrogen atoms from nitrilimine and carbodiimide, forming radical species that could further dissociate to products such as NH (imidogen), methylidyne, N_2 , and the cyano radical. The experimentally observed reaction product ethene could form by the self-reaction of methylene. Formation of the products methane and ammonia may be explained by the very active species methylidyne, methylene, imidogen, and the amino radical (formed via the above reactions) abstracting hydrogen atoms from other less reactive species in the reaction mix. While the above reactions might explain the further reactions of nitrilimine and carbodiimide, it is clear that further work is required to quantify the kinetics of these reaction pathways and to identify subsequent mineralization reactions of the unsaturated nitrogen–hydrocarbon products.

Conclusions

We have examined the thermodynamics and kinetics of five-membered nitrogen-containing heterocycle dissociation according to a retro-[3 + 2]-cycloaddition mechanism, using computational chemistry techniques. Three classes of retro-cycloaddition reactions are identified: class (i) constitutes a simple retro-cycloaddition; class (ii) involves a retro-[3 + 2]-cycloaddition with a concerted intramolecular hydrogen shift; and class (iii) is a multistep mechanism with initial ring opening, followed by a concerted dissociation and hydrogen shift reaction step. Accurate thermochemical properties are reported for the dissociation products $\text{NH}=\text{N}=\text{N}\cdot$, $\text{NH}=\text{N}=\text{CH}$, $\text{NH}=\text{C}=\text{NH}$, $\text{NH}=\text{C}=\text{CH}_2$, acetylene, hydrogen cyanide, and N_2 using the W1 computational method. For dissociation of all the heterocycles, the free energy of activation correlates well with the free energy of reaction, according to a variable-order form of the Marcus equation. The intrinsic activation enthalpy was determined as $37.1 \text{ kcal mol}^{-1}$, with an intrinsic free energy barrier of $42.4 \text{ kcal mol}^{-1}$, but these barriers were found to increase by ca. 32 kcal mol^{-1} when the dissociation reaction involved a concerted intramolecular hydrogen shift, leading to

(43) Prokudin, V. G.; Poplavsky, V. S.; Ostrovskii, V. A. *Russ. Chem. Bull.* **1996**, *45*, 2101.

either $\text{NH}=\text{C}=\text{NH}$ or $\text{NH}=\text{C}=\text{CH}_2$ as one of the products. We calculate rate constants for the processes evaluated in this study between 300 and 3000 K, and find that the retro-[3 + 2]-cycloaddition mechanism should be an important reaction in the decomposition of tetrazole and 1,2,3-triazole. This is confirmed by comparison to experimental results. Decomposition of both tetrazole and 1,2,3-triazole follows a class (iii) mechanism, as defined in this study.

Acknowledgment. We acknowledge the U.S. Army Research Office (Grant Nos. W911NF0410120 and W911NF0710106 administered under Robert Shaw), the New Jersey Institute of

Technology Ada C. Fritts Chair, and ExxonMobil Research and Engineering for partial support of this work.

Supporting Information Available: Geometries (in Cartesian coordinates) and enthalpies (in hartrees) from G3B3 and W1 calculations. Calculated entropies and heat capacities. Intrinsic reaction coordinate (IRC) scans for all dissociation reactions. Plot of reaction free energy versus free energy of activation. Dissociation rate constants as a function of T and P for $300 \text{ K} < T < 3000 \text{ K}$ and $1 \times 10^{-4} \text{ atm} < P < 1 \times 10^3 \text{ atm}$. This material is available free of charge via the Internet at <http://pubs.acs.org>.

JO701914Y